X-ray powder diffraction data for mosapride dihydrogen citrate dihydrate

Analio J. Dugarte-Dugarte [1,a] Robert A. Toro [2] José Antonio Henao [2] Graciela Díaz de Delgado [1] and José Miguel Delgado [1]

[1]*Laboratorio de Cristalografía-LNDRX, Departamento de Química, Facultad de Ciencias, Universidad de los Andes, Mérida 5101, Venezuela*

[2]*Grupo de Investigación en Química Estructural (GIQUE), Escuela de Química, Facultad de Ciencias, Universidad Industrial de Santander, Bucaramanga, Colombia*

(Received 10 March 2024; accepted 14 July 2024)

The previously unindexed laboratory X-ray powder diffraction data of mosapride dihydrogen citrate dihydrate, an API used to stimulate gastrointestinal motility, has been recorded at room temperature. Using these data, the crystal structure of this API has been refined in space group $P2_1/c$ (No. 14) with $a = 18.707(4)$ Å, $b = 9.6187(1)$ Å, $c = 18.2176(4)$ Å, $\beta = 114.164(1)°$, $V = 2990.74(8)$ Å^3, and $Z = 4$. The structure of this material corresponds to the phase associated with CSD Refcode LUWPOL determined at 93 K. The Rietveld refinement, carried out with TOPAS-Academic, proved the single nature of the sample and the quality of the data recorded.

[doi:10.1017/S088571562400040X]

Key words: mosapride dihydrogen citrate dihydrate, X-ray powder diffraction, room temperature, crystal structure, Rietveld refinement

I. INTRODUCTION

Mosapride is a substituted benzamide that is used for its properties of stimulating gastrointestinal motility, helping in the digestion process to clean any residue that may have remained in the esophagus, stomach, and small intestine, without reaching the large intestine (Sweetman, 2009). This drug is administered orally as the citrate dihydrate salt (Figure 1), but doses are expressed as anhydrous citrate.

In the Cambridge Structural Database (CSD) version 2024.1.0 (Groom et al., 2016), there are several reports related to mosapride, one of them is the free base (Refcode: ZEHSEK; Morie et al., 1995) and others correspond to anhydrous mosapride citrate and mosapride dihydrogen citrate dihydrate (Mdcd) (Refcodes: LUWQEC and LUWPOL, respectively; Ito et al., 2020).

The structure determinations of the citrate salts were carried out at 93 K. A few additional reports of mosapride solvates-hydrates were found (Refcodes: GAWVAF, GAWVEJ, GAWVIN, and GAWVOT; Zhang et al., 2022). No reports were found in the PDF-5+ 2024 database (Gates-Rector and Blanton, 2019) of the International Centre for Diffraction Data (ICDD).

Several studies have been published on Mdcd that include, among other characterization techniques, X-ray powder diffraction carried out at room temperature. They report the improvement of the therapeutic effect of tablets using super disintegrates (Ellakwa et al., 2017), the preparation and characterization of inclusion complexes with the aim of improving the solubility and dissolution rate of Mdcd (Ali and Sayed, 2013), and the optimization of solid dispersions (Kim et al., 2011). In these publications, relatively low-quality unindexed X-ray powder diffraction patterns of Mdcd were reported.

Since no data on Mdcd ($C_{21}H_{26}ClFN_3O_3 \cdot C_6H_7O_7 \cdot 2H_2O$, 4-amino-5-chloro-2-ethoxy-*N*-{[(2*RS*)-4-(4-fluorobenzyl)-morpholin-2-yl]methyl}benzamide monocitrate dihydrate, CAS number 636582-62-2) are reported in the ICDD PDF-5 + database (Gates-Rector and Blanton, 2019), the powder diffraction pattern of this pharmaceutical compound has been recorded and analyzed for inclusion in the Powder Diffraction File (PDF) of the ICDD as part of the Grant-in-Aid (GiA) program. This study is part of the research carried out in our laboratories on the identification of pharmaceutical compounds of interest with none or limited structural information reported (Dávila-Miliani et al., 2020; Dugarte-Dugarte et al., 2022, 2023; Toro et al., 2022).

II. EXPERIMENTAL METHODS

A selected specimen of the sample, as provided by Genfar Laboratories, was ground and mounted in a flat sample holder. X-ray powder diffraction data were registered at room temperature on a BRUKER D8 ADVANCE diffractometer with Bragg-Brentano geometry. The pattern was recorded from 4.00° to 70.00° in steps of 0.02035° (2θ) at 1.2 s/step, using Cu $K\alpha$ radiation, operating at 40 kV and 30 mA and a LynxEye detector.

[a]Author to whom correspondence should be addressed. Electronic mail: analio@ula.ve

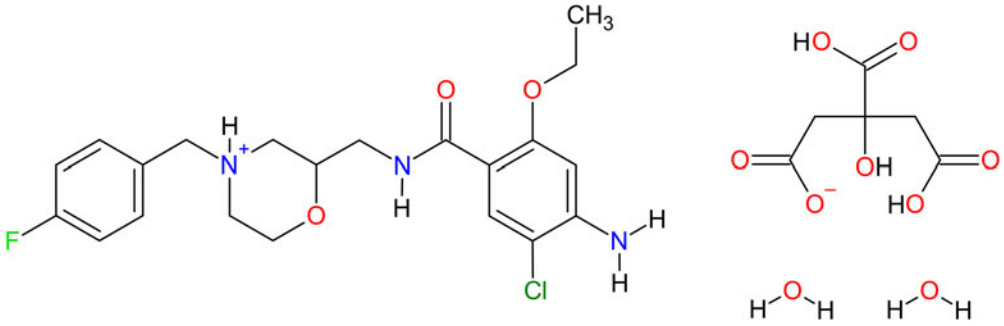

Figure 1. Molecular diagram of mosapride dihydrogen citrate dihydrate (Mdcd).

III. COMPUTATIONAL STUDIES

CrystalExplorer21 software (Spackman et al., 2021) was used to produce "fingerprint plots" of the intermolecular interactions present in the structure. The d_{norm} parameter mapped onto the Hirshfeld surface (Spackman and Jayatilaka, 2009) was calculated to visualize the atoms involved in intermolecular contacts and the strength of such contacts.

IV. RESULTS AND DISCUSSION

The powder pattern recorded has been submitted to the ICDD to be incorporated in the Powder Diffraction File. The indexing of the pattern with DICVOL14 (Louër and Boultif, 2014) as implemented in the PreDICT graphical user interface (Blanton et al., 2019) using the first 20 peaks produced a monoclinic unit cell. The analysis of all the 80 diffraction maxima registered led to the following unit-cell parameters: $a = 18.695(4)$ Å, $b = 9.610(2)$ Å, $c = 18.196(5)$ Å, $\beta = 114.17(2)°$, and $V = 2982.6$ Å^3. The de Wolff (de Wolff, 1968) and Smith-Snyder (Smith and Snyder, 1979) figures of merit obtained were $M_{20} = 15.9$ and $F_{30} = 45.5$ (0.0085, 52), respectively. It must be noted that the cell parameters are similar to the values reported by Ito et al. (2020), indicating that the material under study corresponds to Mdcd.

For the data submitted to the PDF, integrated intensities were obtained by Le Bail refinement (Le Bail et al., 1988) using the FULLPROF software (Rodriguez-Carvajal, 1990). Weak reflections with $I < 0.5\%$ Imax were omitted. The fit led to the following unit-cell parameters: $a = 18.707(4)$ Å, $b = 9.6187(1)$ Å, $c = 18.2176(4)$ Å, $\beta = 114.164(1)°$, and $V = 2990.74(8)$ Å^3.

The superposition of the pattern recorded in the present work with the patterns previously reported (Kim et al., 2011; Ali and Sayed, 2013; Ellakwa et al., 2017) digitized using the online JADE® Pattern Digitizer (ICDD, 2022) are shown in Figure 2. The patterns are similar indicating that all of them correspond to the same Mdcd phase.

Using as a starting structural model the structure reported by Ito et al. (2020), a Rietveld refinement was performed in order to assess the quality of the powder diffraction data recorded. The Pawley fit (Pawley, 1981) of the recorded pattern was carried out by modeling the background, sample displacement errors, absorption, surface roughness, cell parameters, and peak shape parameters (including anisotropic broadening) using TOPAS-Academic (Coelho, 2018). A 15-term Chebyshev polynomial was used to model the background. The intermediate Gaussian–Lorentzian function was employed with a correction for axial divergence as proposed by the program. The surface roughness was modeled using the Pitschke approximation (Pitschke et al., 1993). The

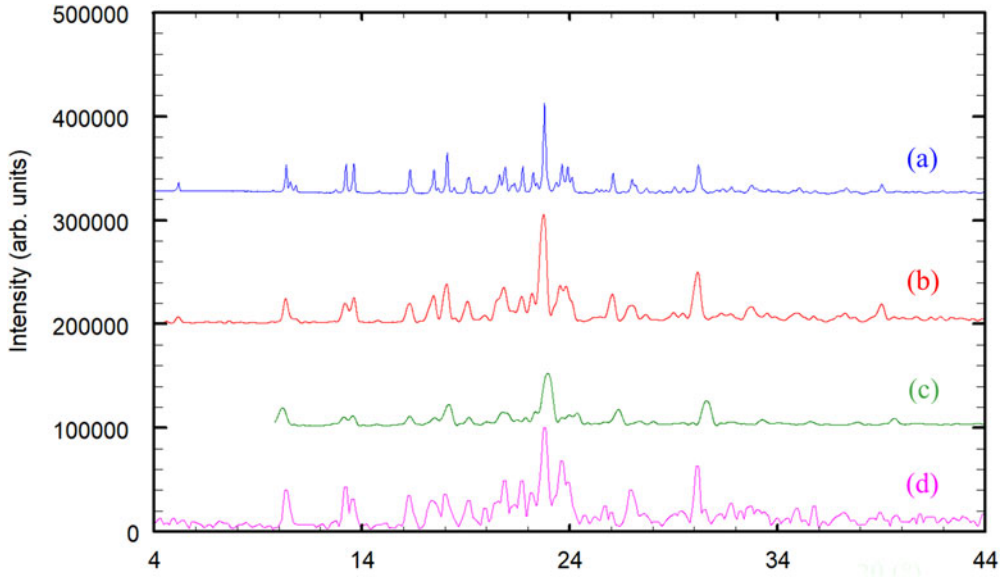

Figure 2. Comparison of the powder pattern recorded for (a) Mdcd in the present study with the reported powder patterns from (b) Ali and Sayed (2013); (c) Kim et al. (2011); and (d) Ellakwa et al. (2017).

https://doi.org/10.1017/S088571562400040X Published online by Cambridge University Press

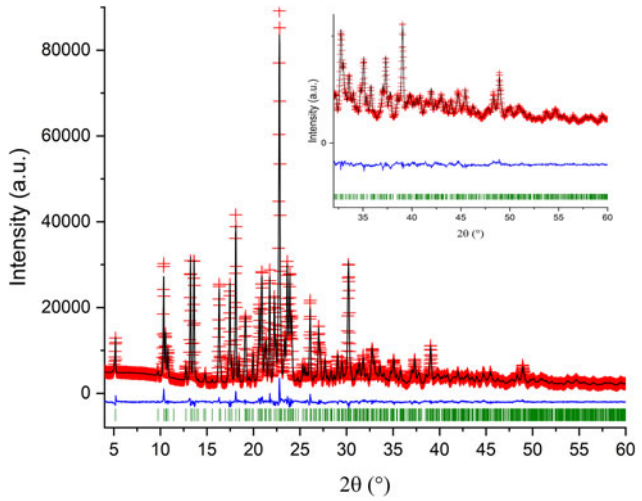

Figure 3. Rietveld refinement plot for Mdcd.

Pawley refinement produced a good fitting of all the diffraction maxima recorded with residuals $R_p = 0.0182$, $R_{wp} = 0.0232$, and GoF = 1.892, confirming the correctness of the unit cell and the single-phase nature of the material. The analysis of the reflection conditions with DASH 4.0.0 (Markvardsen et al., 2001) suggested $P2_1/c$, the same space group determined by Ito et al. (2020).

As mentioned before, the initial structural model, retrieved from CSD entry LUWPOL (Ito et al., 2020), was used for the Rietveld refinement which was carried out with TOPAS-Academic (Coelho, 2018). The refinement included an overall scale parameter, the background, the sample displacement correction, surface roughness corrections, the peak shapes (including anisotropic broadening), unit-cell parameters, absorption correction, atomic coordinates, eight Biso parameters, and a March-Dollase parameter. The bond distances and angles were restrained based on the values suggested by Mogul Geometry Check (Bruno et al., 2004). The weight factors for the distances were 10 000 and 1 for the angles. Four planar restraints, with a standard deviation of 0.01 Å, were applied to the molecule: the C7A-C12A and C16A-C21A aromatic rings, and the O2A-C6A-N2A-HN2 and C10A-N3A-H3N1-H3N2 fragments. The isotropic atomic displacement parameters for the hydrogen atoms were 1.2 times the parameter of the C, N, or O atom to which they are attached.

The refinement performed with TOPAS-Academic (Coelho, 2018) was very stable and proceeded smoothly. Figure 3 shows the final Rietveld refinement plot. In total, 311 parameters were refined with 2753 data points (874 reflections), 217 restraints, and 8 constraints. The final whole pattern fitting converged with good figures of merit: $R_e = 0.0142$, $R_p = 0.0281$, $R_{wp} = 0.0352$, and GoF = 2.473. The March-Dollase preferred orientation parameter (Dollase, 1986) in the (1 0 0) plane was 0.779(1). The excellent fit obtained confirmed that the data recorded are consistent with the structural model obtained from the single crystal diffraction study reported by Ito et al. (2020) for the Mdcd phase. The molecular structure with the corresponding atom labels is presented in Figure 4, drawn with DIAMOND (Putz and Brandenburg, 2023). A CIF file containing this information is in the Supplementary material.

All the bond distances and bond angles fall within the normal ranges as indicated by the Mogul Geometry Check (Bruno et al., 2004). The RMSD calculated with Mercury (Macrae et al., 2020) for 15 molecules, comparing the refined structure with the structure reported in entry LUWPOL, was 0.144 Å.

The structure of Mdcd is governed by extensive hydrogen bonding and displaced face-to-face π···π interactions between the C-rings of two Msp+ molecules. These interactions contribute to the formation of dimers. Hirshfeld surface analysis displays the characteristic red areas corresponding to the hydrogen bonding interactions. The shape index and curvedness representations show the areas of π···π interactions. For the mosapride moiety, H···H and O···H/H···O contacts contribute 40 and 20%, respectively, while for the dihydrogen citrate the O···H/H···O contacts contribute 63.2% and the H···H contacts represent 25.9%.

Details of the structure, the crystal packing, and the crystallochemical analysis carried out are contained in the

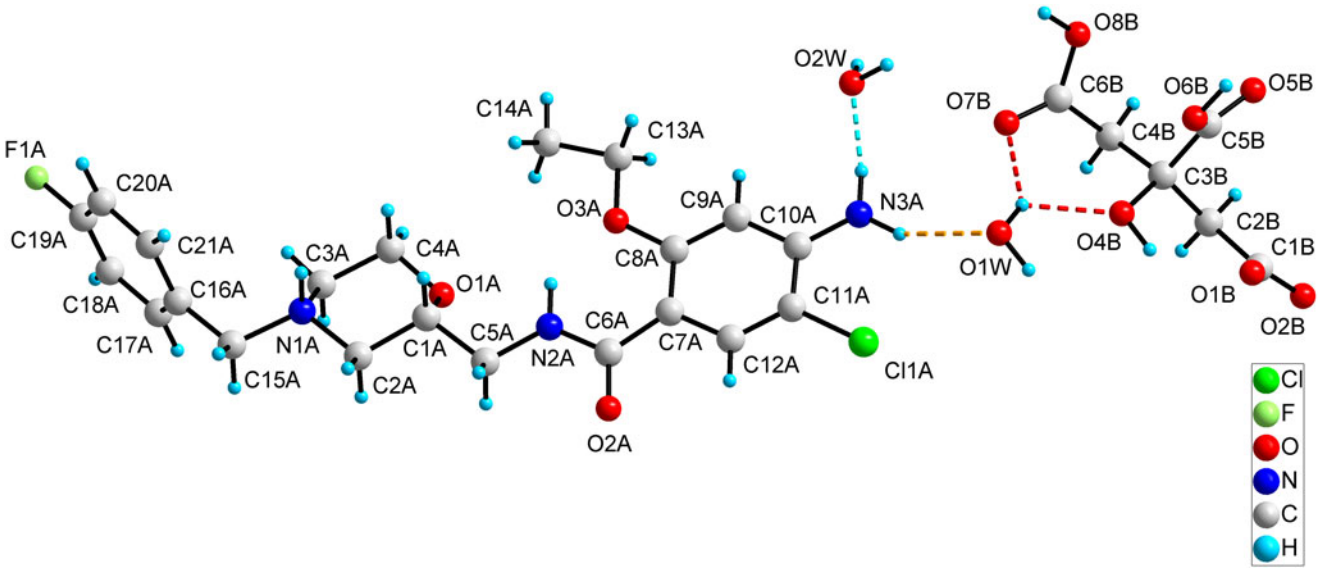

Figure 4. Molecular structure of Mdcd.

https://doi.org/10.1017/S088571562400040X Published online by Cambridge University Press

Supplementary material. This includes tables of bond distances and angles, the most important intermolecular interactions highlighting the hydrogen bonding scheme present, and the Hirshfeld surface and Fingerprint plots calculated for the Msp+, H_2Cit^-, and the water molecules, with the CrystalExplorer21 software (Spackman et al., 2021).

V. DEPOSITED DATA

Crystallographic Information Framework (CIF) files containing the results of the Rietveld refinement and a CIF with the data submitted for the GiA program were deposited with the ICDD. The data can be requested at pdj@icdd.com. The crystal structure data were also deposited with the Cambridge Crystallographic Data Centre (CCDC 2338435).

SUPPLEMENTARY MATERIAL

The supplementary material for this article can be found at https://doi.org/10.1017/S088571562400040X.

ACKNOWLEDGMENTS

The authors thank the support of Vicerrectoría de Investigación y Extensión of Universidad Industrial de Santander (UIS), Colombia. Access to the Cambridge Structural Database (CSD) for Universidad de Los Andes (Venezuela) was possible through the Frank H. Allen International Research & Education Programme (FAIRE) from the Cambridge Crystallographic Data Centre (CCDC).

REFERENCES

Ali, A. A., and O. M. Sayed. 2013. "Preparation and Characterization of Mosapride Citrate Inclusion Complexes with Natural and Synthetic cyclodextrins." *Pharmaceutical Development and Technology* 18 (5): 1042–50. doi:10.3109/10837450.2011.646425.

Blanton, J. R., R. J. Papoular, and D. Louër. 2019. "PreDICT: A Graphical User Interface to the DICVOL14 Indexing Software Program for Powder Diffraction Data." *Powder Diffraction* 34 (3): 233–41. doi:10.1017/S0885715619000514.

Bruno, I. J., J. C. Cole, M. Kessler, J. Luo, W. D. Sam Motherwell, L. H. Purkis, B. R. Smith, R. Taylor, R. I. Cooper, S. E. Harris, and A. Guy Orpen. 2004. Retrieval of Crystallographically-Derived Molecular Geometry Information." *Journal of Chemical Information and Computer Sciences* 44 (6): 2133–44. doi:10.1021/ci049780b.

Coelho, A. A. 2018. "TOPAS and TOPAS-Academic: An Optimization Program Integrating Computer Algebra and Crystallographic Objects Written in C++." *Journal of Applied Crystallography* 51 (1): 210–18. doi:10.1107/S1600576718000183.

Dávila-Miliani, M. C., A. Dugarte-Dugarte, R. A. Toro, J. E. Contreras, H. A. Camargo, J. A. Henao, J. M. Delgado, and G. D. de Delgado. 2020. "Polymorphism in the Anti-Inflammatory Drug Flunixin and Its Relationship with Clonixin." *Crystal Growth and (Design)* 20 (7): 4657–66. doi:10.1021/acs.cgd.0c00284.

de Wolff, P. M. 1968. "A Simplified Criterion for the Reliability of a Powder Pattern Indexing." *Journal of Applied Crystallography* 1 (2): 108–113. doi:10.1107/S002188986800508X.

Dollase, W. A. 1986. "Correction of Intensities for Preferred Orientation in Powder Diffractometry: Application of the March Model." *Journal of Applied Crystallography* 19 (4): 267–72. doi:10.1107/S0021889886089458.

Dugarte-Dugarte, A. J., R. A. Toro, J. van de Streek, J. A. Henao, G. D. de Delgado, and J. M. Delgado. 2022. "Crystal Structure from Laboratory X-Ray Powder Diffraction Data, DFT-D Calculations, and Hirshfeld Surface Analysis of (*S*)-Dapoxetine Hydrochloride." *Powder Diffraction* 37 (4): 216–24. doi:10.1017/S0885715622000380.

Dugarte-Dugarte, A. J., R. A. Toro, J. van de Streek, J. A. Henao, A. N. Fitch, C. Dejoie, J. M. Delgado, and G. D. de Delgado. 2023. "Hydrogen Bonding Patterns and C–H···π Interactions in the Structure of the Antiparkinsonian Drug (*R*)-Rasagiline Mesylate Determined Using Laboratory and Synchrotron X-Ray Powder Diffraction Data." *Acta Crystallographica Section B. Structural Science, Crystal Engineering and Materials* 79 (6): 462–72. doi:10.1107/S2052520623007758.

Ellakwa, T. E., A. Fahmy, and D. E.-S. Ellakwa. 2017. "Influence of Poloxmer on the Dissolution Properties of Mosapride and Its Pharmaceutical Tablet Formulation." *Egyptian Journal of Chemistry* 60 (3): 443–51. doi:10.21608/ejchem.2017.3685.

Gates-Rector, S., and T. Blanton. 2019. "The Powder Diffraction File: A Quality Materials Characterization Database." *Powder Diffraction* 34 (4): 352–60. doi:10.1017/S0885715619000812.

Groom, C. R., I. J. Bruno, M. P. Lightfoot, and S. C. Ward. 2016. "The Cambridge Structural Database." *Acta Crystallographica Section B. Structural Science, Crystal Engineering and Materials* 72 (2): 171–79. doi:10.1107/S2052520616003954.

ICDD. 2022. JADE® Pattern Digitizer. https://www.icdd.com/jade-pattern-digitizer/?page=www.icdd.com/JadeSAS/jade-pattern-digitizer/. Accessed July 14, 2023.

Ito, M., H. Suzuki, and S. Noguchi. 2020. "Chlorine K-Edge X-Ray Absorption Near-Edge Structure Discrimination of Crystalline Solvates and Salts in Organic Molecules." *Crystal Growth and (Design)* 20 (8): 4892–97. doi:10.1021/acs.cgd.0c00790.

Kim, H. J., S. H. Lee, E. A. Lim, and J.-S. Kim. 2011. "Formulation Optimization of Solid Dispersion of Mosapride Hydrochloride." *Archives of Pharmacal Research* 34 (9): 1467–75. doi:10.1007/s12272-011-0908-3.

Le Bail, A., H. Duroy, and J. L. Fourquet. 1988. "Ab-Initio Structure Determination of $LiSbWO_6$ by X-Ray Powder Diffraction." *Materials Research Bulletin* 23 (3): 447–52. doi:10.1016/0025-5408(88)90019-0.

Louër, D., and A. Boultif. 2014. "Some Further Considerations in Powder Diffraction Pattern Indexing with the Dichotomy Method." *Powder Diffraction* 29 (S2): S7–12. doi:10.1017/S0885715614000906.

Macrae, C. F., I. Sovago, S. J. Cottrell, P. T. A. Galek, P. McCabe, E. Pidcock, M. Platings, G. P. Shields, J. S. Stevens, M. Towler, and P. A. Wood. 2020. "Mercury 4.0: From Visualization to Analysis, Design and Prediction." *Journal of Applied Crystallography* 53 (1): 226–35. doi:10.1107/S1600576719014092.

Markvardsen, A. J., W. I. F. David, J. C. Johnson, and K. Shankland. 2001. "A Probabilistic Approach to Space-Group Determination From Powder Diffraction Data." *Acta Crystallographica Section. A. Foundations and Advances* 57 (1): 47–54. doi:10.1107/S0108767300012174.

Morie, T., S. Kato, H. Harada, N. Yoshida, I. Fujiwara, and J.-i. Matsumoto. 1995. "Synthesis and Structure-Activity Relationships of 4-Amino-5-chloro-2-ethoxybenzamides with Six- and Seven-Membered Heteroalicycles as Potential Gastroprokinetic Agents." *Chemical and Pharmaceutical Bulletin* 43 (7): 1137–47. doi:10.1248/cpb.43.1137.

Pawley, G. S. 1981. "Unit-Cell Refinement From Powder Diffraction Scans." *Journal of Applied Crystallography* 14 (6): 357–61. doi:10.1107/S0021889881009618.

Pitschke, W., H. Hermann, and N. Mattern. 1993. "The Influence of Surface Roughness on Diffracted X-Ray Intensities in Bragg–Brentano Geometry and Its Effect on the Structure Determination by Means of Rietveld Analysis." *Powder Diffraction* 8 (2): 74–83. doi:10.1017/S0885715600017875.

Putz, H., and K. Brandenburg. 2023. Diamond-Crystal and Molecular Structure Visualization, Crystal Impact-GbR, Kreuzherrenstr. 102, 53227 Bonn, Germany. https://www.crystalimpact.de/diamond.

Rodriguez-Carvajal, J. 1990. FULLPROF: A Program for Rietveld Refinement and Pattern Matching Analysis." Abstracts of the Satellite Meeting on Powder Diffraction of the XV Congress of the IUCr, Toulouse, France, p. 127.

Smith, G. S., and R. L. Snyder. 1979. "F_N : A Criterion for Rating Powder Diffraction Patterns and Evaluating the Reliability of Powder-Pattern Indexing." *Journal of Applied Crystallography* 12 (1): 60–65. doi:10.1107/S002188987901178X.

Spackman, M. A., and D. Jayatilaka. 2009. "Hirshfeld Surface Analysis." *Crystal Engineering Communications* 11 (1): 19–32. doi:10.1039/B818330A.

Spackman, P. R., M. J. Turner, J. J. McKinnon, S. K. Wolff, D. J. Grimwood, D. Jayatilaka, and M. A. Spackman. 2021. "Crystalexplorer: A Program for Hirshfeld Surface Analysis, Visualization and Quantitative Analysis of Molecular Crystals." *Journal of Applied Crystallography* 54 (3): 1006–11. doi:10.1107/S1600576721002910.

Sweetman, S. C. 2009. *Martindale: The Complete Drug Reference*. 36th ed. Pharmaceutical Press, London, UK.

Toro, R. A., A. Dugarte-Dugarte, J. van de Streek, J. A. Henao, J. M. Delgado, and G. D. de Delgado. 2022. "Crystal Structure From X-Ray Powder Diffraction Data, DFT-D Calculation, Hirshfeld Surface Analysis, and Energy Frameworks of (*RS*)-Trichlormethiazide." *Acta Crystallographica Section E. Crystallographic Communications* 78 (2): 140–48. doi:10.1107/S2056989021013633.

Zhang, B., D. Yang, S. Yang, N. Gong, G. Du, and Y. Lu. 2022. "Preparation, Characterization and Computational Study of Mosapride Solvates." *Journal of Molecular Structure* 1262: 133082. doi:10.1016/j.molstruc.2022.133082.